Inferring DNA sequences from mechanical unzipping: an ideal-case study

V. Baldazzi [1,2,3], S. Cocco [2], E. Marinari [4], R. Monasson [3]
[1] *Dipartimento di Fisica, Università di Roma* Tor Vergata, *Roma, Italy*
[2] *CNRS-Laboratoire de Physique Statistique de l'ENS, 24 rue Lhomond, 75005 Paris, France*
[3] *CNRS-Laboratoire de Physique Théorique de l'ENS, 24 rue Lhomond, 75005 Paris, France*
[4] *Dipartimento di Fisica and INFN, Università di Roma* La Sapienza, *P.le Aldo Moro 2, 00185 Roma, Italy*

We introduce and test a method to predict the sequence of DNA molecules from *in silico* unzipping experiments. The method is based on Bayesian inference and on the Viterbi decoding algorithm. The probability of misprediction decreases exponentially with the number of unzippings, with a decay rate depending on the applied force and the sequence content.

DNA molecules are the support for the genetic information, and knowledge of their sequences is very important from the biological and medical points of view. State-of-the-art DNA sequencing methods rely on biochemical and gel electrophoresis techniques [1], and are able to correctly predict about 99.9% of the bases. They were massively used over the past ten year to obtain the human genome (and the ones of other organisms).

Nevertheless, the quest for alternative (cheaper and/or faster) sequencing methods is an active field of research. In this regard, recent single molecule micromanipulations are of particular interest. Among them are DNA unzipping under a mechanical action [2, 3, 4, 5, 6] or due to translocation through nanopores [7], the observation of the sequence-dependent activity of an exonuclease [8, 9], the optical analysis of DNA polymerization in a nano-chip device [10], the detection of single DNA hybridization [11]. Hereafter, we focus on mechanical unzipping (see Figure 1), first realized by Bockelmann, Heslot and coworkers in 1997 [2, 3]. In their experiment, the strands are pulled apart under a constant velocity. The force is measured and fluctuates around 15 pN for the λ-phage DNA (a $48,502$ base long virus), with higher (respectively, lower) values corresponding to the unzipping of GC (AT) rich regions. Researchers have also unzipped RNA molecules [4, 5, 7], or DNA under a constant force (instead of velocity) [6]. Figure 2A sketches a fixed-force output signal, with its pauses in the opening at sequence-specific positions.

Various theoretical works have studied and reproduced the unzipping signal related to a given sequence [3, 12, 13, 14, 15, 16, 17]. Hereafter we address the inverse problem: given an unzipping signal (for example the one of Figure 2A), can we predict the underlying sequence? We propose a Bayesian inference method to solve this problem [18], and test it *in silico* on the λ-phage. We analytically study the dependence of the quality of the prediction on the sequence content, on the force, and on the number of unzippings. Finally we list the main obstacles to be circumvented prior to practical applications.

Let $\mathcal{S} = \{b_1, b_2, \ldots, b_N\}$ denote the sequence of N bases along the $5' \to 3'$ strand (the other strand is complementary). We model the unzipping of the molecule through the evolution of the number n of open base pairs [13]; base pair opening ($n \to n+1$) and closing

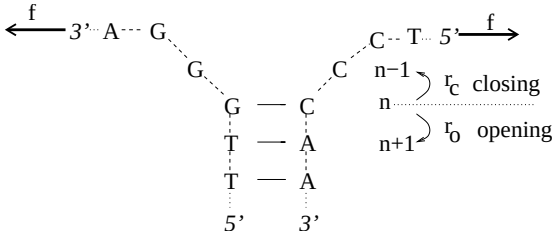

FIG. 1: An unzipping experiment. The extremities of the molecule are stretched apart under a force f. The fork at location n (nb. of open base pairs) moves backward or forward with rates (probability per unit of time) r_c and r_o (1).

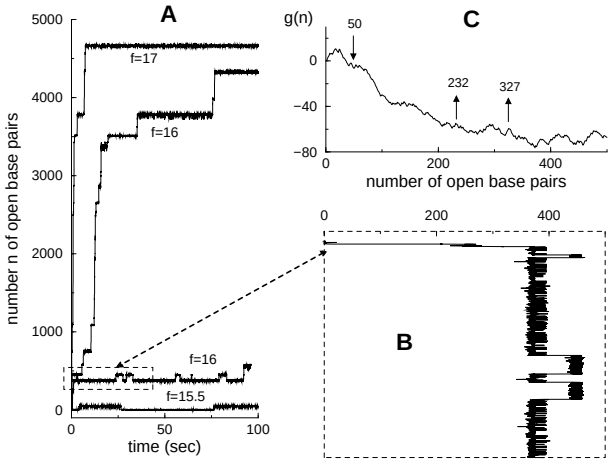

FIG. 2: Fixed-force unzipping of λ-phage. **A.** number n of open base pairs vs. time t for forces f ranging from 15.5 to 17 pN from model (1). **B.** magnification of the boxed region in **A** after a 90 degree clockwise rotation. **C.** free energy landscape $g(n)$ versus n for the first 450 bases and $f = 16$ pN. Down and up arrows indicate, respectively, a local minimum in $n = 50$ and two maxima in $n = 232$ and $n = 327$ (see the text).

($n \to n-1$) happen with rates (Figure 1)

$$r_o(n) = r\ \exp\{g_0(n)\}\ ,\ \ r_c = r\ \exp\{g_{ss}\}\ . \qquad (1)$$

$g_0(n)$ is the binding energy of base pair (bp) n in units of $k_B T$ [19]; it depends on the base $b_n = A, T, G$, or C and, due to stacking effects, on the nearest base b_{n+1}. g_{ss} is

the work needed to stretch an open bp under a force f in units of $k_B T$; according to the modified freely–jointed–chain model [12], $g_{ss} = -2\ell/\ell_0 \ln[\sinh(x)/x]$ where $x \equiv \ell_0 f/k_B T$, and $\ell_0 = 15$ Å and $\ell = 5.6$ Å are, respectively, the Kuhn and effective nucleotide lengths. Relation (1) implies that the opening rate at base n is a function of the sequence, $r_o(n) = r_o(b_n, b_{n+1})$, while the closing rate r_c only depends on the force [20]. This *a priori* choice has been shown [13] to reproduce quantitatively the behavior of unzipping experiments on short polynucleotides [4], with a typical frequency $r \simeq 10^{6-7}$ sec^{-1}.

Rates (1) define a one-dimensional biased random walk for the fork position (number of open bp) $n(t)$ in the potential $g(n) = n\, g_{ss} - \sum_{i=1}^{n} g_0(i)$, that can be interpreted as the free energy of the molecule when the first n bp are open. We show in Figure 2B&C a typical time-trace of $n(t)$ generated by Monte Carlo (MC) simulation for the λ-phage sequence, together with the free energy landscape $g(n)$. Plateaus of $n(t)$ coincide with deep local minima of $g(n)$, where the fork remains trapped for a long time. As the force increases, opening becomes more favorable, and plateaus shrink.

Our *in silico* time-traces are stochastic due to the thermal noise: two runs will give different traces. The probability of a time-trace only depends on the set $\mathcal{N} = \{t_n, u_n, d_n\}$ of times t_n spent on each base n, and of numbers u_n and d_n of up ($n \to n+1$) and down ($n \to n-1$) transitions respectively. Given the sequence $\mathcal{S}$, this probability reads

$$\mathcal{P}(\mathcal{N}|\mathcal{S}) = c \prod_n M(b_n, b_{n+1}; t_n, u_n, d_n) \ , \qquad (2)$$

where c is a (sequence-independent) normalization constant and $M(b_n, b_{n+1}; t_n, u_n, d_n) = r_o\,(b_n, b_{n+1})^{u_n}\ r_c^{d_n}\ \exp\{-(r_o(b_n, b_{n+1}) + r_c)t_n\}$. Equation (2) provides the solution of the direct problem: given the sequence $\mathcal{S}$ what is the distribution of the time-traces $\mathcal{N}$? The inverse problem, that is the prediction of the sequence given some time-trace, can be addressed within the Bayesian inference framework. The probability that DNA sequence is $\mathcal{S}$ given an observed $\mathcal{N}$ is [18]

$$\mathcal{P}(\mathcal{S}|\mathcal{N}) = \frac{\mathcal{P}(\mathcal{N}|\mathcal{S})\ \mathcal{P}_0(\mathcal{S})}{\mathcal{P}(\mathcal{N})} \ . \qquad (3)$$

The value of $\mathcal{S}$ that maximizes this probability, $\mathcal{S}^*$, is our prediction for the sequence. In the absence of any *a priori* information about the sequence, $\mathcal{P}_0(\mathcal{S})$ is the flat distribution, equal to 4^{-N}. The maximization of $\mathcal{P}(\mathcal{S}|\mathcal{N})$ then reduces to that of $\mathcal{P}(\mathcal{N}|\mathcal{S})$ (2).

In practice the most likely sequence $\mathcal{S}^*$ may be found using the Viterbi algorithm [21]. The procedure is equivalent to a zero temperature transfer matrix technique exploiting the nearest-neighbor nature of couplings between bases in (2). The probability P_n for the base b_n fulfills the recursive equation

$$P_{n+1}(b_{n+1}) \propto \max_{b_n}\ P_n(b_n)\, M(b_n, b_{n+1}; t_n, u_n, d_n) \ , \quad (4)$$

where the proportionality constant is irrelevant for our purpose. The maximum in (4) is reached for some base $b_n^{max}(b_{n+1})$ that depends on the next base b_{n+1}. Starting from $P_1(b_1) = \frac{1}{4}$, we obtain the probability $P_N(b_N)$ for the last base of the sequence through iterations of (4). Maximization of $P_N(b_N)$ yields the most likely value for this last base, b_N^*. The whole optimal sequence $\mathcal{S}^*$ is then recursively obtained from the relation $b_{n-1}^* = b_{n-1}^{max}(b_n^*)$.

We have tested our sequencing method on the λ–phage. First we build a dynamical process on the sequence $\mathcal{S}^\lambda$ of the phage with rates (1), and generate an unzipping trace $\mathcal{N}$ by a MC procedure. Then we use the Viterbi procedure (which ignores the phage sequence) to make a prediction for the sequence, $\mathcal{S}^*$, from this signal $\mathcal{N}$. We estimate the error over the prediction about base n from the failure rate

$$\epsilon_n = \text{Probability}\left[b_n^* \neq b_n^\lambda\right] \ , \qquad (5)$$

where the probability is computed by repeating the procedure over different MC runs. The errors ϵ_n are shown in Figure 3 (with the continuous curve) for the first 450 bases at a force of 16 pN. Values range from 0 (perfect prediction) to 0.75 (random guess of one among four bases). A comparison with the free energy $g(n)$ (Figure 2) shows that ϵ_n is small in the flattest part of the landscape ($350 < n < 450$), or in local minima e.g. the $n = 50$ base preceded by 4 weak bases and followed by 4 strong bases (...TTTA-A-GGCG...). Conversely, bases that are not well determined correspond to local maxima of the landscape e.g. $n = 327$, 328 bases between 7 strong and 7 weak bases (...GCCGCCG-TC-ATAAAAT...). We plot the average fraction of mispredicted bases, $\epsilon = \frac{1}{N}\sum_n \epsilon_n$, in Figure 4A. As shown in Fig. 2, for a larger force, there are more open bases (about 60, 600 and 5000 at 15.5, 16 and 17 pN in about 100 seconds), but the time spent on each base is smaller, and therefore ϵ is larger ($\epsilon = 20\%, 23\%, 47\%$). Most errors are due to the difficulty of distinguishing A from T, and G from C. The probability that a weak (A or T) base is confused with a strong one (G or C), or vice-versa, is plotted in Figure 4B.

Performances can be greatly improved by collecting information from multiple unzippings. As the number of passages over the same base n gets larger, the total waiting times t_n and transition parameters u_n, d_n become less affected by fluctuations, and reflect more faithfully the thermodynamic signature of the base. In practice, we look for the most likely sequence $\mathcal{S}^*$ given R unzipping signals $\mathcal{N}_1, \mathcal{N}_2, \ldots, \mathcal{N}_R$. Figures 3A and 4 shows the drop down in the probability of error when the number R of unzippings increases. Observe from Figure 3A that the decay of ϵ_n with R (5) varies from base to base. The

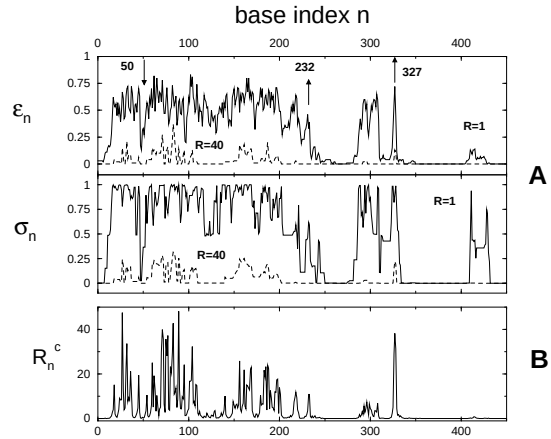

FIG. 3: **A**. Probability ϵ_n of an error (top) and entropy σ_n (middle) versus the base index n, for the first 450 bp of DNA λ-phage at $f = 16$ pN. Full lines correspond to $R = 1$ unzipping, dotted lines to $R = 40$. **B.** Theoretical values for the decay constants R_n^c in ϵ_n (7). For instance, base 232 (arrow) is characterized by $R_{232}^c \simeq 10$, and is not (respectively, well) predicted with $R = 1$ (resp. $R = 40$) unzippings.

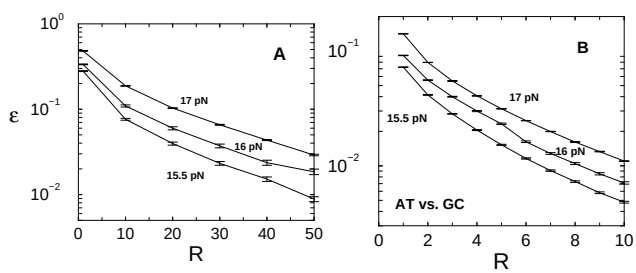

FIG. 4: **A.** Fraction ϵ of mispredicted bases for the λ-phage versus the number R of unzippings, averaged over 1000 samples of R unzippings, and for forces of 15.5, 16 and 17 pN (from bottom to top). **B**. Same as **A**, but we only discriminate among weak and strong basis.

decrease of the total error ϵ is much faster for AT vs. GC (Figure 4B) than for complete (Figure 4A) recognition.

It is useful to build indicators of performances that do not rely on the exact knowledge of the unzipped sequence (used here for checking the quality of our results but unknown in practical applications). To this aim, we calculate the optimal sequences S_b^* when base n is constrained to value b, and the corresponding probabilities $P_n^*(b)$. We then define the Shannon entropy

$$\sigma_n = -\sum_{b=A,T,G,C} \langle P_n^*(b)\, \log_4 P_n^*(b) \rangle \ , \qquad (6)$$

where $\langle \cdot \rangle$ denotes the average over MC data. σ_n is low when one of the four bases has much higher probability than the other ones and close to unity for uncertain predictions (equiprobable bases). Figure 3 shows that σ_n and ϵ_n as a function of the base index n are indeed very similar: the Shannon entropy is a good indicator of the success of our reconstruction.

Our analytical study of the dependence of the quality of the prediction upon the force, the sequence content, and the number of unzippings confirms that the probability of error ϵ_n decreases very quickly with R,

$$\epsilon_n \sim e^{-R/R_n^c} \ . \qquad (7)$$

As f decreases to its critical value (below which the molecule cannot open), the decay constant R_n^c decreases to zero, and predictions drastically improve at fixed R. Our theoretical values for R_n^c are shown in Figure 3B for $f = 16$ pN, and vary from 0.1 to 45 with the base index n. The agreement with the decay of ϵ_n from $R = 1$ to 40 unzippings (Figure 3A) is excellent. Note that ϵ in Figure 4 is not a pure exponential, but a superposition of exponentials with n-dependent decay constants R_n^c. We now present the calculation of R_n^c in three steps.

(a) Pairing only, high force. Assume first that there are only 2 and not 4 bp-types, called + and −, and no stacking interaction. Call Δ the difference between the (pairing) free-energies of + and − bp, and $\langle t_\pm \rangle$ the average time spent by the fork on a $\pm$ bp before moving forward or backward. Consider now a bp of type b and call t the time spent on this bp divided by the number R of unzippings. From the central limit theorem, for large R, t gets narrowly peaked around its mean value $\langle t_b \rangle$, with Gaussian fluctuations $\delta t \sim R^{-\frac{1}{2}}$. Bayes prediction (3) will be erroneous, $b^* = -b$, when t is closer to $\langle t_{-b} \rangle$ than to its expected value $\langle t_b \rangle$. The probability of error is thus given by the Gaussian tail, and scales as $\epsilon \sim \exp(-\delta t^{-2})$, hence (7). A careful calculation [20] gives the precise value of the decay constant in (7),

$$R^c = \frac{1}{\tau - 1 - \ln \tau} \quad \text{with} \quad \tau = \frac{\Delta}{1 - e^{-\Delta}} \ . \qquad (8)$$

Good predictions are obtained when the molecule is unzipped a few R^c times (for example $R \simeq 4R^c$ gives $\epsilon \simeq 2\%$). To distinguish weak (AT) from strong (CG) bp only we have $\Delta \simeq 2.8$ [19] and $R^c \simeq 1$ (Figure 4B), while complete recognition corresponds to $\Delta \simeq 0.5$ and $R^c \simeq 30$ (Figure 4A).

(b) Pairing and Stacking, high force. In presence of stacking interactions, the error ϵ_b on base b depends on the neighboring bases, say, x and y. At large R, errors are rare and are typically due to a single base mis-prediction e.g. $b \to b'$. The probability $\epsilon_{b\to b'}$ of this mistake is the product of the probabilities $\epsilon_{xb\to xb'}$ and $\epsilon_{by\to b'y}$ of the two bond violations. We estimate $\epsilon_{xb\to xb'} \sim e^{-R/R^c_{xb\to xb'}}$ from (7) where $R^c_{xb\to xb'}$ is given by (8) with $\Delta = g_0^{xb'} - g_0^{xb}$. A similar expression is readily obtained for the by bond. Knowing the asymptotic behavior of $\epsilon_{b\to b'}$, we calculate $\epsilon_b \sim e^{-R/R^c_{xby}}$ by selecting the worst value for b',

$$\frac{1}{R^c_{xby}} = \min_{b'(\neq b)} \left[\frac{1}{R^c_{xb\to xb'}} + \frac{1}{R^c_{by\to b'y}} \right] \ . \qquad (9)$$

The above derivation is confirmed by exact calculations based on techniques for 1D disordered systems [20, 22].

(c) Moderate force. The above calculations are correct for high forces. At moderate forces, bp can close and are visited several times by the fork. The effective number of unzippings is $R \times \langle u_n \rangle$, where $\langle u_n \rangle$ is the average number of openings of bp n during a single unzipping. The decay constant is thus, from (7),

$$R_n^c = R^c_{b_{n-1}b_n b_{n+1}} / \langle u_n \rangle \ . \tag{10}$$

As the force is lowered, $\langle u_n \rangle$ increases (from 1 at high force), and R_n^c diminishes. To calculate $\langle u_n \rangle$, we consider the 1D transient random walk defined by the probabilities $q_m \equiv r_c/(r_o(m) + r_c)$ and $1 - q_m$ for closing or opening bp m. Let $p_m^{(n)}$ be the probability that the fork will never reach position n starting from $m(> n)$. The ratios $\rho_m^{(n)} = p_m^{(n)}/p_{m+1}^{(n)}$ fulfill the Riccati recursion relation [20] $\rho_{m+1}^{(n)} = (1 - q_{m+1})/(1 - q_{m+1}\,\rho_m^{(n)})$. Iterating with boundary condition $\rho_n^{(n)} = 0$ allows us to obtain $\langle u_n \rangle = 1/p_n^{(n+1)} = \prod_{m>n} \rho_m^{(n)}$.

Finally we discuss the difficulties hindering a direct application of our inference method to real data (see also [25]), and possible way-outs.

First, temporal resolution is limited in practice. The frequency bandwidth is controlled by the viscous friction and the stiffness of the setup, with a typical value of 10 kHz [3, 24]. The corresponding time, $\delta\tau \simeq 100$ μsec, is about 10 (resp. 200) times longer than the typical opening time for GC (resp. AT) bp. As a result, the fork can move by $D(> 1)$ bp during the time interval $\delta\tau$. We have taken into account such moves by considering interactions between bases at distance $\leq D$ in the probability $P(\mathcal{N}|\mathcal{S})$, and modified the reconstruction procedure accordingly (the transfer matrix has now dimension 4^D) [20]. In practice, when $\delta\tau = 1$ μsec, sequences cannot be predicted with the usual $D = 1$ reconstruction procedure, but are correctly inferred with the $D = 6$ procedure. Though time resolution is currently far below this limit, future experimental progresses, and new technologies e.g. combination of optical trap and single-molecule fluorescence [26], could help bridging the gap.

Secondly, thermal fluctuations of the open strands lead to an uncertainty δn over the position n of the fork [23] e.g. $\delta n \simeq 5$ for $f \simeq 15$ pN and $n = 300$ open bp [12]. The presence of correlations between bases at distance $D \leq \delta n$ does not affect the result (7) for ϵ_n as long as the relaxation time of the strands is smaller than the bp opening time *i.e.* up to a few hundreds open bp. What happens for larger values of n is currently under study.

Thirdly, we have assumed so far to have a perfect knowledge of the dynamics of unzipping. In practice, any functional form for $\mathcal{P}(\mathcal{N}|\mathcal{S})$ will be only approximate for a given experimental setup. A possible way-out based on a learning principle is the following: in a first stage unzipping data corresponding to a known sequence (λ-phage) are collected to caliber $\mathcal{P}$, in a second stage predictions are made for new sequences.

Last of all, our study of fixed-force unzipping shows that bases located in local minima of the free-energy landscape are well predicted, while maxima are much harder to predict. Accuracy could be greatly improved through an adequate force vs. time scheme capable of bringing the fork in the right place and making it spend time there. Investigation of the fixed-velocity case, where the force signal is remarkably affected by single base mutation [3], will be very interesting.

In conclusion, we hope the present study will motivate further work to assess and improve the performances of unzipping-based sequencing.

This work has been partially sponsored by the EC FP6 program under contract IST-001935, EVERGROW, and the French ACI-DRAB & PPF Biophysique-ENS actions.

[1] P.C. Turner, A.G. McLennan, A.D. Bates, M.R.H. White, Molecular Biology, Springer-Verlag (2000).
[2] B. Essevaz-Roulet, U. Bockelmann, F. Heslot, *Proc. Natl. Acad. Sci. (USA)* **94**, 11935 (1997).
[3] U. Bockelmann *et al. Biophys. J.* **82**, 1537 (2002).
[4] J. Liphardt *et al. Science* **297**, 733 (2001).
[5] S. Harlepp *et al. Eur. Phys. J. E* **12**, 605 (2003).
[6] C. Danilowitcz *et al. Proc. Natl. Acad. Sci. (USA)* **100**, 1694 (2003).
[7] J. Mathé *et al. Biophys. J.* **87**, 3205 (2004).
[8] M. van Oijen *et al. Science* **301**, 123 (2003).
[9] T. Perkins *et al. Science* **301**, 1914 (2003).
[10] M.J. Levene *et al. Science* **299**, 682 (2003).
[11] M. Singh-Zocchi *et al. Proc. Natl. Acad. Sci. (USA)* **100**, 7605 (2003).
[12] S. Cocco, R. Monasson, J. Marko. *C.R. Physique* **3**, 569 (2002).
[13] S. Cocco, R. Monasson, J. Marko. *Eur. Phys. J. E* **10**, 153 (2003).
[14] D.K. Lubensky, D.R. Nelson. *Phys. Rev. Lett.* **85**, 1572 (2000); *Phys. Rev. E* **65**, 031917 (2002).
[15] U. Gerland, R. Bundschuh, T. Hwa. *Biophys. J.* **81**, 1324 (2001).
[16] M. Manosas, F. Ritort, *cond-mat/0405035* (2004).
[17] D. Marenduzzo *et al. Phys. Rev. Lett.* **88**, 028102 (2002).
[18] D.H. DeGroot, Probability and Statistics, Addison-Wesley Publishing Co. (1986).
[19] M. Zuker. *Curr. Opin. Struct. Biol.* **10**, 303 (2000). From Santa Lucia Jr. *Proc. Natl. Aca. Sci. (USA)* **95**, 1460 (1998), $g_0^{AA} = -1.78$, $g_0^{AT} = -1.55$, $g_0^{AC} = -2.52$, $g_0^{AG} = -2.22$, $g_0^{TA} = -1.06$, $g_0^{TC} = -2.28$, $g_0^{TG} = -2.54$, $g_0^{CC} = -3.14$, $g_0^{CG} = -3.85$, $g_0^{GC} = -3.90$ k_BT at $T = 25$ C, 150 mM Na.
[20] V. Baldazzi *et al.*, in preparation (2005).
[21] A.J. Viterbi, *IEEE Trans. Inf. Th.* **13**, 260 (1967).
[22] F.J. Dyson *Phys. Rev.* **92**, 1331 (1953).
[23] R.E. Thompson, E.D. Siggia. *Europhys. Lett.* **31**, 335 (1995).
[24] B. Onoa *et al. Science* **299**, 1892 (2003) (supplementary materials).

[25] U. Gerland, R. Bundschuh, T. Hwa. *Phys. Biol.* **1**, 19 (2004).
[26] M.J. Lang, P.M. Fordyce, S.M. Block. *J. Biol.* **2**, 6 (2003).